Inorg. Chem. **2002**, *41*, 2886–2891

Dinuclear (Fe^{II}, Gd^{III}) Complexes Deriving from Hexadentate Schiff Bases: Synthesis, Structure, and Mössbauer and Magnetic Properties

Jean-Pierre Costes,* Juan Modesto Clemente-Juan, Françoise Dahan, Frédéric Dumestre, and Jean-Pierre Tuchagues

Laboratoire de Chimie de Coordination du CNRS, UPR 8241, Liée par Conventions à l'Université Paul Sabatier et à l'Institut National Polytechnique de Toulouse, 205 Route de Narbonne, 31077 Toulouse Cedex, France

Received December 14, 2001

The dinuclear (Fe^{II}, Gd^{III}) complexes studied in this report derive from hexadentate Schiff base ligands abbreviated H_2L^i (i = 1, 2, 3). H_2L^1 = *N*,*N*′-bis(3-methoxysalicylidene)-1,3-diamino-2,2′-dimethyl-propane, H_2L^2 = *N*,*N*′-bis(3-methoxysalicylidene)-1,2-diamino-2-methylpropane, and H_2L^3 = *N*,*N*′-bis(3-methoxysalicylidene)-1,2-diaminoethane. The crystal and molecular structures of three complexes have been determined at 160 K. Depending on the solvent used in the preparation, $L^1Fe(CH_3OH)Gd(NO_3)_3(CH_3OH)_2$, **1**, or $L^1Fe((CH_3)_2CO)Gd(NO_3)_3$, **1′**, is obtained from H_2L^1. A similar complex, $L^2Fe((CH_3)_2CO)Gd(NO_3)_3$, **2**, is obtained from H_2L^2. Complex **1** crystallizes in the orthorhombic space group *Pca*2$_1$ (No. 29): a = 22.141(3) Å, b = 9.4159(16) Å, c = 15.2075(17) Å, V = 3170.4(7) Å^3, Z = 4. Complexes **1′** and **2** crystallize in the monoclinic space group $P2_1/c$ (No. 14): **1′**, a = 9.6264(17) Å, b = 19.662(3) Å, c = 16.039(3) Å, β = 95.15(2)°, V = 3023.6(9) Å^3, Z = 4; **2**, a = 9.7821(13) Å, b = 18.7725(17) Å, c = 16.100(2) Å, β = 96.497(16)°, V = 2937.5(6) Å^3, Z = 4. Complexes **1**, **1′**, and **2** possess an $Fe(O_{phenoxo})_2$-Gd core. The mononuclear L^3Fe complex could be prepared from H_2L^3 but not the related dinuclear (Fe, Gd) species. Mössbauer spectroscopy evidences that the iron center is in the +2 oxidation state for the six complexes. The experimental magnetic susceptibility and magnetization data of complexes **1**, **1′**, and **2** indicate the occurrence of weak Fe^{II}–Gd^{III} ferromagnetic interactions. Single ion zero-field splitting of the iron(II) must be taken into account for satisfactorily fitting the data by exact calculation of the energy levels associated to the spin Hamiltonian through diagonalization of the full matrix for axial symmetry (**1**, J = 0.50 cm^{-1}, D = 2.06 cm^{-1}; **1′**, J = 0.41 cm^{-1}, D = 3.22 cm^{-1}; **2**, J = 0.08 cm^{-1}, D = 4.43 cm^{-1}).

Introduction

Several studies aimed at evaluating the nature and magnitude of the magnetic interaction between a paramagnetic lanthanide ion (Ln) and a second spin carrier (M) have been performed.[1−8] However, they are doubly restricted because, very generally, the 4f ion is Gd^{III} and the second center is either an organic radical or a Cu^{II} ion. Very few bimetallic (M, Gd) complexes in which M is different from Cu^{II} have been reported; they concern VO^{II},[9] Ni^{II}_{hs},[10] Co^{II},[11] Cr^{III},[12] Fe^{II},[13] and Fe^{III}.[14] Until recently, all (M, Gd) compounds that have an M−Gd interaction and for which a

* To whom correspondence should be addressed. E-mail: costes@lcc-toulouse.fr. Phone: 33(0)561333152. Fax: 33(0)561553003.

(1) (a) Bencini, A.; Benelli, C.; Caneschi, A.; Carlin, R. L.; Dei, A.; Gatteschi, D. *J. Am. Chem. Soc.* **1985**, *107*, 8128.
(2) Decurtins, S.; Gross, M.; Schmalle, H. W.; Ferlay, S. *Inorg. Chem.* **1998**, *37*, 2443.
(3) (a) Andruh, M.; Ramade, I.; Codjovi, E.; Guillou, O.; Kahn, O.; Trombe, J. C. *J. Am. Chem. Soc.* **1993**, *115*, 1822. (b) Ramade, I.; Kahn, O.; Jeannin, Y.; Robert, F. *Inorg. Chem.* **1997**, *36*, 930. (c) Daiguebonne, C.; Guillou, O.; Kahn, M. L.; Kahn, O.; Oushoorn, R. L.; Boubekeur, K. *Inorg. Chem.* **2001**, *40*, 176.
(4) (a) Chen, X. M.; Aubin, S. M. J.; Wu, Y. L.; Yang, Y. S.; Mak, T. C. W.; Hendrickson, D. N. *J. Am. Chem. Soc.* **1995**, *117*, 9600. (b) Chen, X. M.; Wu, Y. L.; Tong, Y. X.; Huang, X. Y. *J. Chem. Soc., Dalton Trans.* **1996**, 2443.
(5) (a) Costes, J. P.; Dahan, F.; Dupuis, A.; Laurent, J. P. *Inorg. Chem.* **1997**, *36*, 3429. (b) Costes, J. P.; Dahan, F.; Dupuis, A.; Laurent, J. P. *Inorg. Chem.* **2000**, *39*, 165.
(6) Stemmler, A. J.; Kampf, J. W.; Kirk, M. L.; Atasi, B. H.; Pecoraro, V. L. *Inorg. Chem.* **1999**, *38*, 2807.
(7) Sanz, J. L.; Ruiz, R.; Gleizes, A.; Lloret, F.; Faus, J.; Julve, M.; Borras-Almenar, J. J.; Journaux, Y. *Inorg. Chem.* **1996**, *35*, 7384.
(8) Liu, Q. D.; Gao, S.; Li, J. R.; Zhou, Q. Z.; Yu, K. B.; Ma, B. Q.; Zhang, S. W.; Zhang, X. X.; Jin, T. Z.. *Inorg. Chem.* **2000**, *39*, 2488.
(9) (a) Costes, J. P.; Dahan, F.; Donnadieu, B.; Garcia-Tojal, J.; Laurent, J. P. *Eur. J. Inorg. Chem.* **2001**, 363. (b) Costes, J. P.; Dupuis, A.; Laurent, J. P. *J. Chem. Soc., Dalton Trans.* **1998**, 735.

10.1021/ic0112793 CCC: $22.00
Published on Web 05/04/2002

detailed analysis of the magnetic properties was available have been shown to exhibit a ferromagnetic interaction between the two spin carriers. In the case of the (Cu, Gd) pair, a theoretical approach[3a] has attributed this behavior to a mechanism involving simultaneously ground and excited states of the bimetallic couple. Nevertheless, ferromagnetism cannot be considered as an intrinsic property of the (M, Gd) couple. Very recent papers point to the existence of a few (M, Gd) complexes (M = Cu^{II},[15] VO^{II},[9] organic radical[16,17]) with an antiferromagnetic ground state: it would thus be important to develop a more sophisticated model of interaction including simultaneously antiferromagnetic and ferromagnetic contributions. To increase the range of M centers among the (M, Gd) dinuclear systems, we have considered the case of the Fe^{II} ion. A first example of discrete (Fe^{II}, Gd^{III}) complexes has previously been published where the two metal centers do not interact significantly because they are far from each other and not directly linked by a material bridge.[13,18] The present contribution describes the structure and magnetic properties of three bimetallic (Fe^{II}, Gd^{III}) complexes obtained from the mononuclear L^iFe^{II} (i = 1, 2) precursors. The H_2L^i ligands (Figure 1) have already been employed to prepare various (M, Gd) complexes.[5,9,10c] The mononuclear L^3Fe complex is also described, but we have not been able to isolate the related dinuclear (Fe, Gd) species.

Experimental Section

Materials and Methods. All starting materials were purchased from Aldrich and used without further purification. $Fe(CH_3COO)_2 \cdot 2H_2O$,[19] L^1H_2,[5] L^2H_2,[5] and L^3H_2[20] were obtained as previously described. The preparation of complexes pertaining to the same series (L^iFe^{II} or $Fe^{II}L^iGd^{III}$) being similar, the experimental procedure will only be described for the first complex in each series. All complexation reactions and sample preparations for physical measurements were carried out in a purified nitrogen atmosphere within a glovebox (Vacuum Atmospheres H. E.43.2) equipped with a dry-train (Jahan EVAC 7).

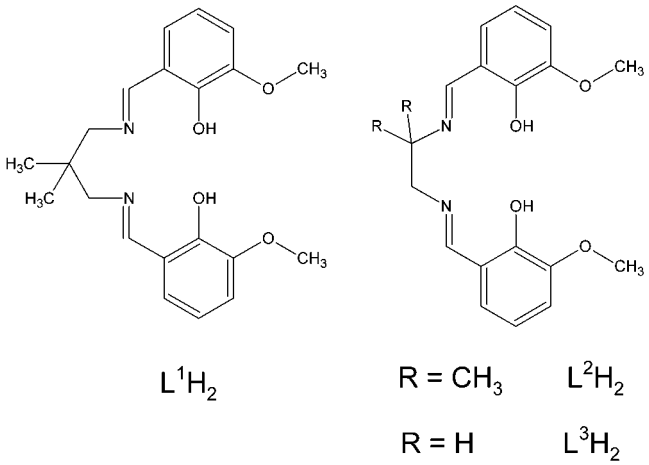

Figure 1. Ligands used in the present work.

$L^1Fe(MeOH)(H_2O)$. A mixture of orthovanillin (1.0 g, 6.6 × 10^{-3} mol) and 1,3-diamino-2,2-dimethylpropane (0.34 g, 3.3 × 10^{-3} mol) in methanol (10 mL) was stirred for 10 min. Then, $Fe(CH_3COO)_2 \cdot 2H_2O$ (0.69 g, 3.3 × 10^{-3} mol) was added as a solid, yielding a reddish solution which was stirred for 15 h at room temperature. A maroon precipitate was filtered off and washed with a minimum amount of cold methanol. Yield: 1.25 g (82%). Anal. Calcd for $C_{22}H_{30}FeN_2O_6$: C, 55.7; H, 6.4; N, 5.9. Found: C, 55.5; H, 6.1; N, 5.8. Characteristic IR absorptions (KBr, cm^{-1}): 3423m (ν_{OH}), 1607s ($\nu_{C=N}$).

The experimental procedure is identical for L^2Fe and L^3Fe, except that these Schiff base ligands were isolated prior to complexation.

$L^2Fe(MeOH)(H_2O)$. Yield: 0.74 g (60%). Anal. Calcd for $C_{21}H_{28}FeN_2O_6$: C, 54.8; H, 6.1; N, 6.1. Found: C, 54.9; H, 6.2; N, 5.9. Characteristic IR absorptions (KBr, cm^{-1}): 3427m (ν_{OH}), 1603s ($\nu_{C=N}$).

$L^3Fe(2H_2O)$. Yield: 1.03 g (84%). Anal. Calcd for $C_{18}H_{22}FeN_2O_6$: C, 51.7; H, 5.3; N, 6.7. Found: C, 51.5; H, 4.9; N, 6.9. Characteristic IR absorptions (KBr, cm^{-1}): 3436m (ν_{OH}), 1601s ($\nu_{C=N}$).

$[L^1Fe(CH_3OH)Gd(NO_3)_3]$ (1). An excess of $Gd(NO_3)_3 \cdot 6H_2O$ (0.65 g, 1.5 × 10^{-3} mol) was added to a suspension of $L^1Fe(MeOH)(H_2O)$ (0.50 g, 1.1 × 10^{-3} mol) in methanol (7 mL). Stirring induced a quick dissolution of the mononuclear complex. The resulting green precipitate was filtered off 10 h later and washed with methanol. Yield: 0.74 g (89%). Anal. Calcd for $C_{22}H_{28}FeGdN_5O_{14}$: C, 33.0; H, 3.5; N, 8.8. Found: C, 33.0; H, 3.2; N, 8.7. Characteristic IR absorptions (KBr, cm^{-1}): 3412m (ν_{OH}), 1615s ($\nu_{C=N}$), 1476s, 1301s, 1285s (ν_{NO3}).

$[L^1Fe((CH_3)_2CO)Gd(NO_3)_3]$ (1′). Using acetone instead of methanol yielded again a green powder analyzing as $L^1Fe(CH_3COCH_3)Gd(NO_3)_3$.Yield: 0.54 g (65%). Anal. Calcd for $C_{24}H_{30}FeGdN_5O_{14}$: C, 34.9; H, 3.7; N, 8.5. Found: C, 34.7; H, 3.4; N, 8.4. Characteristic IR absorptions (KBr, cm^{-1}): 1675m ($\nu_{C=O}$),-1610s ($\nu_{C=N}$), 1474s, 1302s, 1279s (ν_{NO3}).

$[L^2Fe((CH_3)_2CO)Gd(NO_3)_3]$ (2). Red powder. Yield: 0.54 g (69%). Anal. Calcd for $C_{23}H_{28}FeGdN_5O_{14}$: C, 34.0; H, 3.5; N, 8.6. Found: C, 33.7; H, 3.3; N, 8.4. Characteristic IR absorptions (KBr, cm^{-1}): 1673m ($\nu_{C=O}$), 1608s ($\nu_{C=N}$), 1463s, 1313s, 1279s (ν_{NO3}).

Crystallographic Data Collection and Structure Determination for 1, 1′, and 2. Crystals suitable for X-ray analyses were obtained by slow evaporation of the corresponding solutions (methanol for **1** or acetone for **1′** and **2**) inside the glovebox. The

(10) (a) Brechin, E. K.; Harris, S. G.; Parsons, S.; Winpenny, R. E. P. *J. Chem. Soc., Dalton Trans.* **1997**, 1665. (b) Winpenny, R. E. P. *Chem. Soc. Rev.* **1998**, *27*, 447. (c) Costes, J. P.; Dahan, F.; Dupuis, A.; Laurent, J. P. *Inorg. Chem.* **1997**, *36*, 4284. (d) Lisowski, J.; Starynowicz, P. *Inorg. Chem.* **1999**, *38*, 1351.
(11) (a) Costes, J. P.; Dahan, F.; Dupuis, A.; Laurent, J. P. *C. R. Acad. Sci., Ser. IIc: Chim.* **1998**, *1*, 417. (b) Brayshaw, P. A.; Bünzli, J.-C. G.; Froidevaux, P.; Harrowfield, J. M.; Kim, Y.; Sobolev, A. N. *Inorg. Chem.* **1995**, *34*, 2068. (c) Rigault, S.; Piguet, C.; Bernardinelli, G.; Hopfgartner, G. *J. Chem. Soc., Dalton Trans.* **2000**, 4587. (d) Ma, B. Q.; Gao, S.; Bai, O.; Sun, H. L.; Xu, G. X. *J. Chem. Soc., Dalton Trans.* **2000**, 1003.
(12) Sanada, T.; Suzuki, T. ; Yoshida, T.; Kaizaki, S. *Inorg. Chem.* **1998**, *37*, 4712.
(13) Edder, C.; Piguet, C.; Bünzli, J.-C. G.; Hopfgartner, G. *Chem.—Eur. J.* **2001**, *7*, 3014.
(14) Costes, J. P.; Dupuis, A.; Laurent, J. P. *Eur. J. Inorg. Chem.* **1998**, 1543.
(15) (a) Costes, J. P.; Dahan, F.; Dupuis, A.; Laurent, J. P. *Inorg. Chem.* **2000**, *39*, 169. (b) Costes, J. P.; Dahan, F.; Dupuis, A.; Laurent, J. P. *Inorg. Chem.* **2000**, *39*, 5994.
(16) Lescop, C.; Luneau, D.; Belorisky, E.; Fries, P.; Guillot, M.; Rey, P. *Inorg. Chem.* **1999**, *38*, 5472.
(17) Caneschi, A.; Dei, A.; Gatteschi, D.; Sorace, L.; Vostrikova, K. *Angew. Chem., Int. Ed.* **2000**, *39*, 246.
(18) (a) Piguet, C.; Rivara-Minten, E.; Hopfgartner, G.; Bünzli, J.-C. G. *Helv. Chim. Acta* **1995**, 78, 1651. (b) Piguet, C.; Rivara-Minten, E.; Bernardinelli, G.; Bünzli, J.-C. G.; Hopfgartner, G. *J. Chem. Soc., Dalton Trans.* **1997**, 421.
(19) Rhoda, N.; Fraioli, A. V. *Inorg. Synth.* **1953**, *159*, 4.
(20) Guerriero, P.; Tamburini, S.; Vigato, P. A.; Russo, U.; Benelli, C. *Inorg. Chim. Acta* **1993**, *213*, 279.

Table 1. Crystallographic Data for $L^1Fe(CH_3OH)Gd(NO_3)_3(CH_3OH)_2$ (**1**), $L^1Fe((CH_3)_2CO)Gd(NO_3)_3$ (**1′**), and $L^2Fe(CH_3OH)Gd(NO_3)_3$ (**2**)

	1	**1′**	**2**
formula	$C_{24}H_{36}FeGdN_5O_{16}$	$C_{24}H_{30}FeGdN_5O_{14}$	$C_{23}H_{28}FeGdN_5O_{14}$
fw	863.68	825.63	811.60
space group	$Pca2_1$ (No. 29)	$P2_1/c$ (No. 14)	$P2_1/c$ (No. 14)
a, Å	22.141(3)	9.6264(17)	9.7821(13)
b, Å	9.4159(16)	19.662(3)	18.7725(17)
c, Å	15.2075(17)	16.039(3)	16.100(2)
β, deg		95.15(2)	96.497(16)
V, Å^3	3170.4(7)	3023.6(9)	2937.5(6)
Z	4	4	4
ρ_{calcd}, g cm^{-3}	1.809	1.814	1.835
λ, Å	0.71073	0.71073	0.71073
T, K	160	160	160
μ(Mo Kα) cm^{-1}	26.12	27.30	28.08
$R_{(obs, all)}$[a]	0.0278, 0.0305	0.0193, 0.0213	0.0229, 0.0269
$R_{w(obs, all)}$[b]	0.0687, 0.0703	0.0445, 0.0452	0.0505, 0.0542

[a] $R = \sum||F_o| - |F_c||/\sum|F_o|$. [b] $R_w = [\sum[w(|F_o|^2 - |F_c|^2)^2]/\sum w|F_o^2|^2]^{1/2}$.

selected crystals of **1** (light green parallelepiped, 0.50 × 0.45 × 0.20 mm^3), **1′** (light-brown parallelepiped, 0.50 × 0.40 × 0.30 mm^3), and **2** (dark-red plate, 0.45 × 0.15 × 0.10 mm^3) were mounted on a Stoe imaging plate diffractometer system (IPDS) using a graphite monochromator (λ = 0.71073 Å) and equipped with an Oxford Cryosystems cooler device. The data were collected at 160 K. The crystal-to-detector distance was 80 mm (max 2θ value 48.4°). Data were collected[21] with a φ rotation movement for **1** and **1′** (φ = 0.0°−229.5°, $\Delta\varphi$ = 1.5° for **1** and φ = 0.0°−214.2°, $\Delta\varphi$ = 1.4° for **1′**) and with a φ oscillation movement for **2** (φ = 0.0°−212.8°, $\Delta\varphi$ = 1.4°). There were 22390 reflections collected for **1**, of which 5008 were independent (R_{int} = 0.0559), 20456 reflections for **1′**, of which 4656 were independent (R_{int} = 0.0311), and 19549 reflections for **2**, of which 4552 were independent (R_{int} = 0.0334). Numerical absorption corrections[22] were applied. Maximum and minimum transmission factors were 0.6831 and 0.3150 for **1**, 0.8210 and 0.5756 for **1′**, and 0.6639 and 0.1942 for **2**, respectively. The structures were solved by direct methods using SHELXS-97[23] and refined by full-matrix least-squares on F_o^2 with SHELXL-97.[24] In **2**, the disordered C atoms of the $NC(CH_3)_2CH_2N$ ring were refined with 0.5 occupancy factors. All non-hydrogen atoms were refined anisotropically. H atoms were introduced in calculations by using the riding model with U_{iso} = 1.1U_{iso}(atom of attachment). The atomic scattering factors and anomalous dispersion terms were taken from the standard compilation.[25] The maximum and minimum peaks on the final difference Fourier map were 0.940 and −0.479 e Å^{-3} for **1**, 0.804 and −0.508 e Å^{-3} for **1′**, and 1.049 and −0.827 e Å^{-3} for **2**, respectively. Drawings of the molecules were performed with the program ZORTEP.[26] Crystal data collection and refinement parameters are given in Table 1, and selected bond distances and angles are gathered in Table 2.

Table 2. Selected Bond Lengths (Å), Distances (Å), and Angles (deg) for Complexes **1**, **1′**, and **2**

	1	**1′**	**2**
$Fe-O(1)_{phenolato}$	2.027(3)	2.031(2)	1.975(2)
$Fe-O(2)_{phenolato}$	2.019(3)	2.030(2)	1.942(2)
Fe−N(1)	2.069(4)	2.074(2)	2.009(2)
Fe−N(2)	2.082(3)	2.066(2)	2.008(2)
Fe−O(5)	2.055(4)	2.123(2)	2.113(2)
$Gd-O(1)_{phenolato}$	2.348(3)	2.388(2)	2.362(2)
$Gd-O(2)_{phenolato}$	2.328(3)	2.381(2)	2.393(2)
$Gd-O(3)_{methoxy}$	2.529(3)	2.561(2)	2.618(2)
$Gd-O(4)_{methoxy}$	2.534(4)	2.539(2)	2.623(2)
$Gd-O_{nitrato}$	2.464(4)−2.572(4)	2.464(2)−2.547(2)	2.447(2)−2.534(2)
Gd−O(1)−Fe	106.3(1)	105.19(7)	103.55(7)
Gd−O(2)−Fe	107.3(1)	105.46(7)	103.49(7)
O(1)−Fe−O(2)	79.1(1)	78.0(6)	81.4(7)
O(1)−Gd−O(2)	66.9(1)	64.8(5)	65.0(6)
α[a]	6.2(7)	23.6(1)	24.1(1)
Gd···Fe	3.5057(5)	3.5169(4)	3.4152(4)

[a] Dihedral angle between the O−Gd−O and O−Fe−O planes of the bridging network.

Physical Measurements. Elemental analyses were carried out at the Laboratoire de Chimie de Coordination Microanalytical Laboratory in Toulouse, France, for C, H, and N. IR spectra were recorded on a GX system 2000 Perkin-Elmer spectrophotometer. Samples were run as KBr pellets.

Mössbauer measurements were obtained on a constant-acceleration conventional spectrometer with a 50 mCi source of ^{57}Co (Rh matrix). Isomer shift values (δ) throughout the paper are given with respect to metallic iron at room temperature. The absorber was a sample of 100 mg of microcrystalline powder enclosed in a 20 mm diameter cylindrical plastic sample-folder, the size of which had been determined to optimize the absorption. Variable-temperature spectra were obtained in the 80−200 K range, by using a MD 306 Oxford cryostat, the thermal scanning being monitored by an Oxford ITC4 servocontrol device (±0.1 K accuracy). A least-squares computer program[27] was used to fit the Mössbauer parameters and determine their standard deviations of statistical origin (given in parentheses).

Magnetic data were obtained with a Quantum Design MPMS SQUID susceptometer. All samples were 3 mm diameter pellets molded in the glovebox from ground crystalline samples. Magnetic susceptibility measurements were performed in the 2−300 K temperature range in a 0.7 T applied magnetic field, and diamagnetic corrections were applied by using Pascal's constants.[28] Isothermal magnetization measurements as a function of the external magnetic field were performed up to 5 T at 2 K. The magnetic susceptibility has been computed by exact calculation of the energy levels associated to the spin Hamiltonian through diagonalization of the full matrix with a general program for axial symmetry,[29] and with the MAGPACK program package[30] in the case of magnetization. Least-squares fittings were accomplished with an adapted version of the function-minimization program MINUIT.[31]

(21) *STOE, IPDS Manual*. Version 2.93; Stoe and Cie: Darmstadt, Germany, 1997.

(22) *Stoe, X-SHAPE. Crystal Optimisation for Numerical Absorption Corrections*, Revision 1.01; Stoe and Cie: Darmstadt, Germany, 1996.

(23) Sheldrick, G. M. *SHELXS-97. Program for Crystal Structure Solution*; University of Göttingen: Göttingen, Germany, 1990.

(24) Sheldrick, G. M. *SHELXL-97. Program for the refinement of crystal structures from diffraction data*; University of Göttingen: Göttingen, Germany, 1997.

(25) *International Tables for Crystallography*; Kluwer Academic Publishers: Dordrecht, The Netherlands, 1992; Vol. C.

(26) Zsolnai, L.; Pritzkow, H.; Huttner, G. *ZORTEP. Ortep for PC, Program for Molecular Graphics*; University of Heidelberg: Heidelberg, Germany, 1996.

(27) Varret, F. Proceedings of the International Conference on Mössbauer Effect Applications; Jaipur, India, 1981; Indian National Science Academy: New Delhi, 1982.

(28) Pascal, P. *Ann. Chim. Phys.* **1910**, *19*, 5.

(29) (a) Garge, P.; Chikate, R.; Padhye, S.; Savariault, J.-M.; de Loth, P.; Tuchagues, J.-P. *Inorg. Chem.* **1990**, *29*, 3315. (b) Aussoleil, J.; Cassoux, P.; de Loth, P.; Tuchagues, J.-P. *Inorg. Chem.* **1989**, *28*, 3051.

(30) (a) Borrás-Almenar, J. J.; Clemente-Juan, J. M.; Coronado, E.; Tsukerblat, B. S. *Inorg. Chem.* **1999**, *38*, 6081. (b) Borrás-Almenar, J. J.; Clemente-Juan, J. M.; Coronado, E.; Tsukerblat, B. S. *J. Comput. Chem.* **2001**, *22*, 985−991.

Results and Discussion

Syntheses. The synthetic pathway comprises two steps, the first one leading to the mononuclear iron(II) precursor and the second one to the related dinuclear (Fe^{II}, Gd^{III}) complex. All complexes were prepared in a glovebox under a purified nitrogen atmosphere. In agreement with previous results,[5] the Fe^{II} ion enters into the inner N_2O_2 coordination site of the ligand while the oxophilic Gd^{III} ion occupies the O_4 outer site. The process is effective when the ligand is H_2L^1 or H_2L^2. Incidentally, it may be noted that the precise structure of the final product depends on the solvent used during the preparation and/or recrystallization. In the case of H_2L^1, two complexes, $L^1Fe(CH_3OH)Gd(NO_3)_3$, **1**, and L^1-$Fe((CH_3)_2CO)Gd(NO_3)_3$, **1′**, have been isolated and structurally characterized (see later). In the case of H_2L^3, the second step of the reaction failed to afford the expected dinuclear complex but led to a powder which, according to the analytical and spectroscopic data, does not contain any bimetallic (Fe^{II}, Gd^{III}) species. It shall be noted that the L^3-Fe precursor was prepared without any problem and isolated in high yield. All compounds were characterized by chemical analyses, IR, and ^{57}Fe Mössbauer spectroscopy.

Description of the Structures. Complexes **1** and **1′** deriving from the same polydentate ligand crystallize in different crystallographic systems, orthorhombic (space group $Pca2_1$) and monoclinic ($P2_1/c$), respectively, while complex **2** crystallizes in the same space group as **1′**, suggesting that the crystallographic system depends on the volume of the solvent molecule apically coordinated to the iron center. In all three complexes, the unit cell contains four neutral dinuclear species $L^iFe(D)Gd(NO_3)_3$ (D = CH_3OH (**1**) or $(CH_3)_2CO$ (**1′**, **2**); i = 1 (**1**, **1′**) and 2 (**2**)). Additional methanol molecules are present in the case of complex **1**: they are not coordinated but involved in intramolecular hydrogen bonds.

The three $L^iFe(D)Gd(NO_3)_3$ molecular units exhibit very similar features. They are illustrated in Figures 2 and 3 for complexes **1** and **2**, respectively. Relevant structural parameters for the three structures are gathered in Table 2. The core of each molecular unit is built up from two metal ions, Fe^{II} and Gd^{III}, doubly bridged by two phenolato oxygen atoms of L^i, O(1) and O(2). The Fe, O(1), O(2), Gd core is not planar: the dihedral angle α between the [O(1)FeO(2)] and [O(1)GdO(2)] planes shows that departure from planarity of the Fe, O(1), O(2), Gd core is significantly larger in **1′** (α = 23.6(1)°) and **2** (α = 24.1(1)°) compared to **1** (α = 6.2(7)°). Gd^{III} is decacoordinated with four oxygen atoms from the phenolato groups and the methoxy sidearms of the L^i ligand and six oxygen atoms from three bidentate nitrato anions. The distortion of the coordination polyhedron around Fe^{II} can be quantified using the approach of Muetterties and Guggenberger.[32] In this method, the dihedral angles between adjacent faces (known as shape-determining angles e_1, e_2, and e_3) are calculated in order to describe an intermediate geometry. The key shape-determining angle, e_3, is equal to 0° for an ideal square pyramid and 53.1° for an ideal trigonal bipyramid. The e_3 angle is equal to 1.1° for the Fe^{II} site in **1** and **2** and 3.5° for the Fe^{II} site in **1′**, confirming that the coordination of Fe^{II} is square pyramidal with a solvent molecule at the apex. The basal N_2O_2 donors provided by L^i are almost coplanar. The larger deviations are equal to 0.033(2) Å in **1′** and 0.010(3) Å in **1** and **2**. The Fe^{II} ion is displaced from the mean N_2O_2 plane by 0.3434(9) Å and 0.3558(3) Å toward the axial O(5) oxygen atom for **1** and **1′**, respectively, while this displacement is larger in **2** (0.4935(3) Å). The axial Fe−O(5) bond lengths are in the 2.055(4)−2.123(2) Å range, larger than their basal Fe−O(1,2) counterparts (1.942(2)−2.031(2) Å). The Fe−N(1,2) distances are in the 2.008(2)−2.082(3) Å range.[33] As usual, the Gd−O bond lengths[5,9,10c,15] depend on the nature of the oxygen atom: in the three complexes, the shortest bond distances correspond to the phenolato oxygens (average:

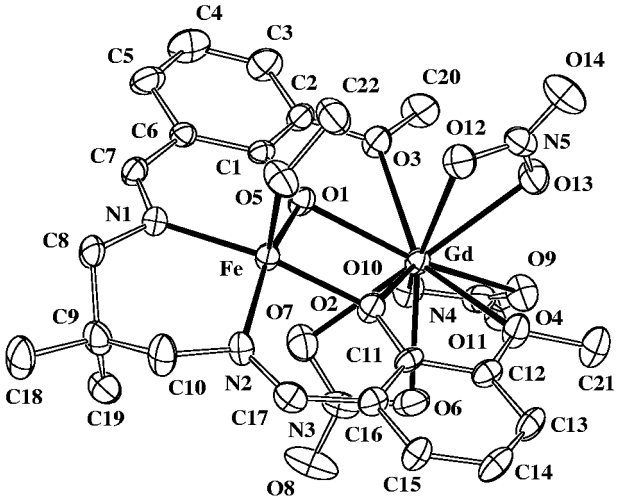

Figure 2. Zortep view of complex **1** with ellipsoids drawn at the 50% probability level.

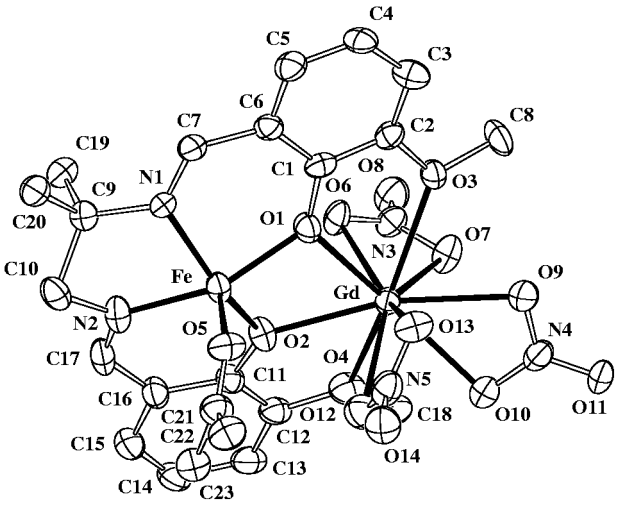

Figure 3. Zortep view of complex **2** with ellipsoids drawn at the 50% probability level.

(31) James, F.; Roos, M. MINUIT Program, a System for Function Minimization and Analysis of the Parameters Errors and Correlations. *Comput. Phys. Commun.* **1975**, *10*, 345.

(32) Muetterties, E. L.; Guggenberger, L. J. *J. Am. Chem. Soc.* **1974**, *96*, 1748.

(33) Corazza, F.; Floriani, C.; Zehnder, M. *J. Chem. Soc., Dalton Trans.* **1987**, 709.

Table 3. Mössbauer Parameters for Complexes $L^1Fe{\cdot}MeOH{\cdot}H_2O$, $L^2Fe{\cdot}MeOH{\cdot}H_2O$, $L^3Fe{\cdot}2H_2O$, $L^1Fe(CH_3OH)Gd(NO_3)_3$ (**1**), $L^1Fe((CH_3)_2CO)Gd(NO_3)_3$ (**1′**), and $L^2Fe(CH_3OH)Gd(NO_3)_3$ (**2**)

cmpd	T (K)	δ (mms^{-1})[a]	ΔE_Q (mms^{-1})	$\Gamma/2$ (mms^{-1})[b]
$L^1Fe{\cdot}MeOH{\cdot}H_2O$	80	1.099(1)	2.464(2)	0.120(2)
$L^2Fe{\cdot}MeOH{\cdot}H_2O$	80	1.000(1)	2.410(2)	0.128(2)
$L^3Fe{\cdot}2H_2O$	80	1.045(1)	2.496(1)	0.135(1)
1	80	1.059(1)	2.609(2)	0.116(2)
1	90	1.055(2)	2.604 (4)	0.115(3)
1	100	1.044(3)	2.596 (6)	0.113(5)
1	140	1.033(2)	2.565 (4)	0.110(3)
1	160	1.019(2)	2.541 (4)	0.118(3)
1	180	1.014(1)	2.523 (2)	0.113(2)
1	200	0.996(1)	2.487 (2)	0.110(1)
1′	80	1. 140 (2)	3.368(4)	0.206(4)
2	80	0.922(2)	2.491(3)	0.170(2)

[a] Isomer shift referenced to metallic iron at room temperature. [b] Width at half-height.

2.367 Å) and the largest ones to the methoxy groups (average: 2.515 Å). The parameters gathered in Table 3 show that, despite their overall similarity, the three complexes display structural differences: basal Fe−O and Fe−N bond lengths are larger in **1** and **1′** than in **2**; a similar trend is observed for the intramolecular Gd···Fe separations and Gd−O(1,2)−Fe angles while the larger Gd−O(1,2) and axial Fe−O(5) bond lengths occur in complex **1′**.

The intermolecular metal−metal distances (7.610(1)−9.416(1) Å) are much larger than the intramolecular Fe···Gd ones (3.4152(4)−3.5169(4) Å), clearly indicating that complexes **1**, **1′**, and **2** may be considered as genuine examples of strictly dinuclear (Fe^{II}, Gd^{III}) species.

Mössbauer Spectroscopy. Mössbauer spectra of the three L^iFe precursors and the related dinuclear $L^iFe(D)Gd(NO_3)_3$ complexes collected in the 80−200 K range consist of a single quadrupole split doublet. They were least-squares fitted with Lorentzian lines, and the resulting isomer shift (δ) and quadrupole splitting (ΔE_Q) parameters (Table 3) are consistent with high-spin Fe^{II} sites. At 80 K, the range of δ values for the L^iFe precursors (1.000−1.099 mms^{-1}) is consistent with their similar octahedral coordination spheres including the equatorial N_2O_2 donor set from the L^i Schiff base and two apical O donors from solvent molecules (MeOH and/or H_2O); the range of ΔE_Q values (2.410−2.496 mms^{-1}) is consistent with a significant and similar distortion of the N_2O_4 coordination octahedron in these related mononuclear precursors.

The crystal structures of complexes **1**, **1′**, and **2** evidence that Fe^{II} experiences a N_2O_2 + O square pyramidal ligand environment in the dinuclear $L^iFe(D)Gd(NO_3)_3$ species, at variance with its octahedral coordination in the mononuclear precursors. This significant difference is clearly observed on comparing the Mössbauer parameters at 80 K. The change in Fe^{II} coordination from $N_2O_2 + O_{MeOH} + O_{H2O}$ ($L^1Fe(MeOH)(H_2O)$ and ($L^2Fe(MeOH)(H_2O)$) to $N_2O_2 + O_{MeOH}$ (**1**) and $N_2O_2 + O_{Acetone}$ (**1′** and **2**) is accompanied by an increase in ΔE_Q (from 2.464 to 2.609 (**1**) and 3.368 mms^{-1} (**1′**) and from 2.410 to 2.491 mms^{-1} (**2**)) in agreement with an increased axial distortion.[34] The ΔE_Q value for complex **1′** at 80 K (3.368 mms^{-1}) is significantly larger than those for **1** and **2** (2.609 and 2.491 mms^{-1}, respectively), indicating that the departure from cubic symmetry is essentially axial in the case of complex **1′** while the symmetry is lower than axial for **1** and **2**. This is in agreement with the differences in structural parameters characterizing the N_2O_2 + O square pyramidal ligand environment of Fe^{II} in complexes **1**, **1′**, and **2**. The effects on δ values are more subtle: because of the change from the N_2O_4 to N_2O_3 donor set around Fe^{II} centers, a decrease in δ is expected as observed on comparing the δ values obtained at 80 K for the mononuclear (1.000 mms^{-1}) and dinuclear (0.922 mms^{-1}) complexes involving the L^2 ligand. Comparison of the δ values obtained at 80 K for $L^1Fe(MeOH)(H_2O)$ and **1** shows also a slight decrease, while a slight increase is observed on comparing $L^1Fe(MeOH)(H_2O)$ and **1′**.

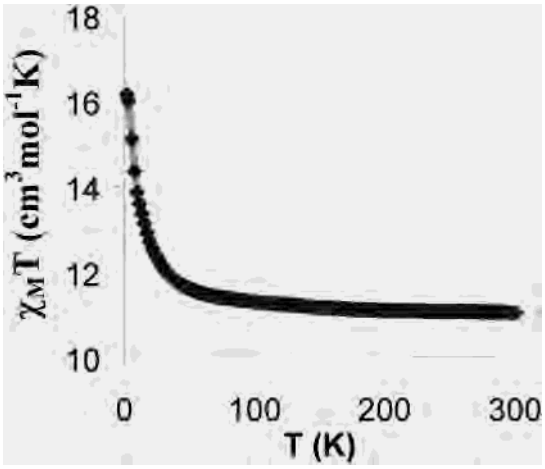

Figure 4. Thermal dependence of $\chi_M T$ for complex **1′**. The solid line represents the best fit of the data with the model including single Fe^{II} ion ZFS (see text).

Mössbauer parameters of the iron(II) site of complex **1** obtained at different temperatures are also collected in Table 3. As expected, the δ values are slightly temperature dependent because of the second-order Doppler shift.[34] The ΔE_Q values are almost independent of temperature (2.609 (80 K)−2.487 mms^{-1} (200 K)), indicating that the separation between the ground state and the higher orbital states is large enough to preclude thermal population of the later.

Magnetic Properties. The magnetic susceptibility χ_M of complexes **1**, **1′**, and **2** has been measured in the 2−300 K temperature range in a 0.7 T applied magnetic field, while isothermal magnetization measurements as a function of the external magnetic field were performed up to 5 T at 2 K. The data obtained for complex **1′** are represented in Figure 4. At 300 K, the $\chi_M T$ product is equal to 11.10 cm^3 mol^{-1} K, which is slightly larger than the expected 10.87 cm^3 mol^{-1} K value for noninteracting $S = 2$ (Fe) and $S = {}^7/_2$ (Gd) spins. As the temperature is lowered, $\chi_M T$ gradually increases, indicating the presence of a ferromagnetic interaction; very similar data were obtained for **1**. In the case of complex **2**, the $\chi_M T$ product is constant from room temperature to 40 K with a $\chi_M T$ value equal to 11.28 cm^3 mol^{-1} K. When the sample is further cooled, $\chi_M T$ increases, up to a maximum around 6 K with a $\chi_M T$ value of ∼11.8 cm^3 mol^{-1} K, and

(34) Greenwood, N. N.; Gibb, T. C. *Mössbauer Spectroscopy*; Chapman and Hall: London, 1971.

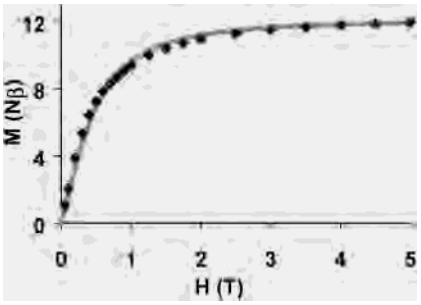

Figure 5. Field dependence of the magnetization for complex **1** at 2 K. The solid line represents the data computed with the sets of exchange and ZFS parameters obtained from the best fit of the $\chi_M T$ curve shown in Figure 5 (see text).

then slightly decreases. It shall be emphasized that these small $\chi_M T$ variations originate exclusively from the insulated dinuclear units constituting complexes **1**, **1′**, and **2**. Because of the orbital degeneracy of high-spin iron(II) ($S = 2$), application of an isotropic spin Hamiltonian is not rigorous for these complexes. The Kotani expressions,[35] appropriate with isolated iron(II) centers, are not suitable here because of the Fe−Gd magnetic interaction. The exchange phenomenon in the presence of orbital degeneracy is an open problem for which no general solution is available. Also, as discussed by one of us,[36] the orbital contribution is significantly quenched when the iron(II) environment deviates from ideal octahedral geometry. This is the case of complexes **1**, **1′**, and **2** where the iron(II) centers are pentacoordinated with a square pyramidal geometry; in such a case, the orbital degeneracy can affect only weakly the temperature dependence of the $\chi_M T$ product.[37,38] Attempts to fit the data by using the simplified $H = -2JS_{Fe}S_{Gd}$ Hamiltonian failed, indicating that zero field splitting (ZFS) of iron(II) cannot be neglected. The energy levels and magnetic properties of spin systems including the anisotropic iron(II) usually require consideration of single ion ZFS terms. This ZFS term includes the anisotropy originating from the orbital contribution. The simpler spin Hamiltonian that may be used is $H = -2JS_{Fe}S_{Gd} + D_{Fe}S_z^2{}_{Fe} + \sum_i j\ g_i\beta H_j S_{ij}$ in which the first term gauged by the parameter J accounts for the spin exchange interaction, the second one gauged by D accounts for axial single ion ZFS of iron(II), and the third one accounts for the Zeeman contributions where $i =$ Fe, Gd and $j = x, y, z$. The temperature dependence of $\chi_M T$ was fitted using the described Hamiltonian. Analytical expressions for eigenvalues and susceptibility cannot be derived because of the ZFS term. To calculate the energy levels and magnetic properties, diagonalization of the full matrix has been carried out.[29] The best fits for complexes **1**, **1′**, and **2** (as illustrated in Figure 4 for **1′**) were obtained for the following sets of parameters, the g values of the low-lying states being combinations of g_{Fe} and g_{Gd}:[39] **1**, $J = 0.50$ cm^{-1}, $D = 2.06$ cm^{-1}, $g_{Fe} = 2.182$, $g_{Gd} = 2.000$; **1′**, $J = 0.41$ cm^{-1}, $D = 3.22$ cm^{-1}, $g_{Fe} = 2.006$, $g_{Gd} = 2.000$; **2**, $J = 0.08$ cm^{-1}, $D = 4.43$ cm^{-1}, $g_{Fe} = 2.100$, $g_{Gd} = 2.000$.

The 2 K magnetization data were then satisfactorily simulated with these sets of parameters (as illustrated in Figure 5 for **1′**) confirming simultaneous operation of ferromagnetic Fe−Gd exchange interactions and single Fe^{II} ion ZFS: all energy levels corresponding to the sets of exchange and ZFS parameters obtained from the fits of the susceptibility curves have been taken into account, and diagonalization of the full matrix has been performed at each value of the magnetic field for calculation of the theoretical magnetizations.[30a]

Consideration of Figures 4 and 5 shows that the model deriving from the aforementioned Hamiltonian is appropriate to account for the magnetic behavior of the (Fe^{II}, Gd^{III}) pairs. The occurrence of a ZFS term, the magnitude D of which is similar or larger to that of the exchange parameter J, is responsible for the atypical profiles of the $\chi_M T$ versus T plots. The M versus H experimental data can be correctly fitted only if the ZFS term D is taken into account (Figure 5).

In a previous work,[5b] it has been shown for (Cu, Gd) pairs that the sign and magnitude of the exchange interaction are dependent on the bending of the (CuO_2Gd) core gauged by the dihedral angle, α. Seemingly, this interpretation does not hold in the present work. Indeed, the J values for complexes **1** and **1′** are very similar in sign and magnitude while the corresponding α values (Table 2) differ significantly. On the contrary, almost identical α values are observed for **1** and **2** which display different J values. This situation may originate from operation of two antagonist effects in the present complexes, that is, ferromagnetic interaction and single Fe^{II} ion ZFS. Considering that the exchange mechanism is also affected by the increased number of active d electrons (from one (Cu^{II}) to four (Fe^{II})), additional examples are needed to substantiate this hypothesis.

Acknowledgment. We thank Dr. A. Mari for his contribution to the magnetic measurements. The authors are greatly indebted to Dr. J. P. Laurent for fruitful discussion. The European Community is acknowledged for partial support through a postdoctoral grant to J.M.C.-J. within the framework of TMR Contract FMRX- CT980174.

Supporting Information Available: Additional figures and X-ray crystallographic files including the structural data for [L^1-$Fe(CH_3OH)Gd(NO_3)_3](CH_3OH)_2$ (**1**), [$L^1Fe(CH_3COCH_3)Gd(NO_3)_3$] (**1′**), and [$L^2Fe(CH_3COCH_3)Gd(NO_3)_3$] (**2**) in CIF format. This material is available free of charge via the Internet at http://pubs.acs.org.

IC0112793

(35) Kotani, M. *J. Phys. Soc. Jpn.* **1949**, *4*, 293.
(36) Borras-Almenar, J. J.; Clemente-Juan, J. M.; Coronado, E.; Palii, A. V.; Tsukerblat, B. S. *J. Phys. Chem. A* **1998**, *102*, 200.
(37) Carlin, R. L. *Magnetochemistry*; Springer-Verlag: New York, 1986.
(38) *Theory and Applications of Molecular Magnetism*; Boudreaux, E. A., Mulay, L. N., Eds.; Wiley-Interscience: New York, 1976.
(39) Bencini, A.; Gatteschi, D. *EPR of Exchange Coupled Systems*; Springer-Verlag: Berlin, 1990.